TIC 308396022: a δ Scuti–γ Doradus hybrid with large-amplitude fundamental radial mode and regular g-mode period spacing

Tao-Zhi Yang[1], Zhao-Yu Zuo[1], Gang Li[2], Timothy R Bedding[3,4], Simon J Murphy[3,4], Meridith Joyce[5]

ABSTRACT

We analyse the pulsating behaviour of TIC 308396022 observed by the TESS mission, which is a high-amplitude δ Sct star (HADS). The star shows a very rich amplitude spectrum using the 3-yr light curve. Among these frequencies, the strongest peak of $p_1 = 13.20362567(12)\,\mathrm{d}^{-1}$ is identified as the fundamental radial mode, and we also find the first and second overtones (p_2 and p_3). In the low frequency range ($< 2.5\ \mathrm{d}^{-1}$), 22 peaks are identified to be gravity modes, which show a regular period spacing of about 2460 s and have the angular degree $l = 1$. The period spacing pattern does not show a significant downward trend, suggesting the star rotates slowly. We note that this is the first δ Sct–γ Dor hybrid star containing a high-amplitude fundamental radial mode (HADS) and a regular g-mode period spacing pattern. With O-C analysis, we find the star shows a significant time delay, implying that the star has a companion which is likely to be a white dwarf. The history of possible mass transfer provides a great opportunity to test the current theories of binary evolution, mass transfer, and pulsation.

Subject headings: stars: oscillations; stars: variable: delta Scuti; individual: TIC 308396022

---

[1] Ministry of Education Key Laboratory for Nonequilibrium Synthesis and Modulation of Condensed Matter, School of Physics, Xi'an Jiaotong University, 710049 Xi'an, PR China; *e-mail:zuozyu@xjtu.edu.cn (ZYZ);

[2]IRAP, Université de Toulouse, CNRS, CNES, UPS, Toulouse, France;

[3]Sydney Institute for Astronomy (SIfA), School of Physics, University of Sydney, Camperdown NSW 2006, Australia

[4]Stellar Astrophysics Centre, Department of Physics and Astronomy, Aarhus University, Ny Munkegade 120, DK-8000 Aarhus C, Denmark

[5]Space Telescope Science Institute in Baltimore, MD, USA;

1. Introduction

The study of stellar oscillations is a powerful tool to probe the internal structures of stars by using stellar periodic oscillations (Aerts et al. 2010; Chaplin & Miglio 2013; Catelan & Smith 2015; Aerts 2021). Oscillations can be observed photometrically (Handler 2013; Aerts 2021) and pulsation frequencies can be found by calculating the amplitude spectrum (e.g. Lomb 1976; Scargle 1982). After that, many parameters, such as mass, age, rotation, and distance can be measured, which are not straightforward to observe otherwise.

A class of short-period pulsating stars, δ Sct stars, shows great potential for asteroseismic studies. They are intermediate-mass variables with spectral types between A2 and F2, and situated in the lower end of the classical instability strip (Breger 2000; Murphy et al. 2019). Most δ Sct stars are multi-periodic pulsators and may show radial and non-radial pulsations (Bowman 2017). These pulsations are driven by the κ mechanism operating in the He-II partial ionization zone (Breger 2000; Aerts et al. 2010), therefore the pulsations are low-radial-order (n) low-angular-degree (l) pressure (p) modes with periods between 15 minutes and 8 hours (Uytterhoeven et al. 2011; Holdsworth et al. 2014). Their masses are generally between $1.5M_{\odot}$ and $2.5M_{\odot}$, which place them in the transition regime between low-mass stars with convective envelope and high-mass stars with radiate envelope and convective core (Bowman 2017). Thus, the pulsations in δ Sct star provide the opportunity to make detailed studies of stellar structure and evolution in this transition regime (Bowman & Kurtz 2018).

However, the amplitude spectra of δ Sct stars are generally very rich and messy, which challenges the mode identification (Goupil et al. 2005; Handler 2009). Recently, Bedding et al. (2020) found that some young multi-periodic δ Sct stars show regular frequency separations as predicted by the asymptotic relation (Shibahashi 1979; Tassoul 1980), providing a new possibility for asteroseismology in δ Sct stars. In addition, there is a sub-class δ Sct stars named high-amplitude δ Sct stars (HADS), whose mode identification is relatively clear. The HADS usually pulsate in the fundamental radial mode and in radial overtones, with amplitudes of about 0.1 magnitude (Petersen 1989; Petersen & Christensen-Dalsgaard 1996). The target in this work, TIC 308396022, is a HADS.

A- to F-type main-sequence stars may also pulsate in gravity (g) modes. These are known as γ Dor stars, which appear near the red edge of the δ Sct instability strip and show low-frequency light variations (Balona, Krisciunas & Cousinset 1994; Kaye et al. 1999; Dupret et al. 2005). These stars have typical masses from 1.4 to 2.0 $M_{\odot}$ (e.g. Kaye et al. 1999; Van Reeth et al. 2016), and they usually pulsate in low-degree high-order g modes driven by the convective blocking mechanism (Guzik et al. 2000; Dupret et al. 2004, 2005), with periods between 0.2 days and 2 days and typical amplitudes below 0.01 mag (Li et al. 2020). The g modes sometimes show uniform spacings in period, as predicted by the asymptotic relation, but deviations from the uniform period

spacing patterns appear, which reveal the physics of the stellar interior, such as chemical component gradients (Miglio et al. 2008), near-core rotation rates (Bouabid et al. 2013; Ouazzani et al. 2017), and coupling between g modes and inertial modes (Ouazzani et al. 2020; Saio et al. 2021).

The overlapping of the instability strips of δ Sct and γ Dor stars allows the existence of hybrid stars that show both p- and g-mode pulsations (Breger & Beichbuchner 1996). The g modes carry the information of the near-core region and the p modes can probe the stellar envelope (Grigahcène et al. 2010; Kurtz et al. 2014; Saio et al. 2015), so the hybrid pulsators of δ Sct and γ Dor stars have great potential to study the internal structure of a star. Several δ Sct–γ Dor hybrid stars have been detected by ground-based observations (Handler & Shobbrook 2002; Henry & Fekel 2005; Handler 2009), and the large number observed by space missions such as *CoRoT* (Baglin et al. 2009) and *Kepler* (Borucki et al. 2010) suggested that hybrid behavior might be common in A-F stars (Grigahcène et al. 2010; Hareter et al. 2010). Based on a large sample (750 stars) of δ Sct and γ Dor candidates discovered in Kepler mission, Uytterhoeven et al. (2011) found that about 63% (471 stars) of the sample show δ Sct or γ Dor pulsations, and 36% (171 stars) are hybrid δ Sct–γ Dor stars. Recent studies (e.g. Bradley et al. 2015) with a larger sample of δ Sct–γ Dor stars suggest that hybrid stars are very common. With the successful launch of TESS mission (Ricker et al. 2014, 2015), more hybrid stars will be found and hence provide better understanding of this kind of variable.

TIC 308396022 (TYC 8928-1300-1; α_{2000}=$08^h01^m02^s.370$, δ_{2000}=$-63°40'30''.317$) was first observed in the Sector 1 of the TESS observations and classified to be a pulsating star in Antoci et al. (2019). Its basic properties from that study and the TESS Input Catalogue (TIC; Stassun et al. 2018) are listed in Table 1. To investigate the pulsations of TIC 308396022 further, we analyse the 2-min cadence photometric data spanning three years from the TESS mission.

2. Observation and Data Reduction

TIC 308396022 was observed in Sectors 1, 4, 5, 7 to 11 during the first cycle of the TESS mission, and again in Sectors 27, 28, 31, 34, 35, 37, 38 during Cycle 3. We use all these light curves, which are available from the Mikulski Archive for Space Telescopes (MAST) [1]. We downloaded all the data and used the 2-min cadence Simple Aperture Photometry (SAP) light curves for our research. In each sector, the obvious outliers were removed and the slow trend was corrected with a high pass filter. In total, the rectified light curve includes 236991 data points spanning 1035 days with a duty-cycle of 32%. Figure 1 shows the phased light curve, folded by the dominant frequency

[1]MAST: http://archive.stsci.edu/

Table 1. Basic parameters of TIC 308396022.

Parameters	TIC 308396022	References
TESS magnitude	11.069	a
alternative ID	GSC 08928-01300	a
	2MASS J08010239-6340302	
$T_{\rm eff}$	6730 ± 248 K	(Gaia), a
	6860 ± 150 K	SED, b
	7371 ± 150 K	SED, c
log g	3.81 ± 0.25 dex	(Gaia, phot), a
	4.12 ± 0.25 dex	c
log $(L/L_{\odot})$	0.94 ± 0.01	(Gaia), a
Parallax (mas)	1.71 ± 0.02	(Gaia), a
B	11.55	c
V	10.997	c
J	10.573	c
H	10.471	c
K	10.371	c
Gaia mag	11.330	a

Note. — (a) Gaia (McDonald et al. 2017). (b) Antoci et al. (2019). (c) Parameters from the TESS Input Catalogue (Stassun et al. 2018): https://tasoc.dk/catalog/.

$p_1 = 13.20362567(12)\,\mathrm{d}^{-1}$. The peak-to-peak amplitude of the dominant mode is $\sim 14.7\%$.

3. Frequency Analysis and Mode Identification

To extract the pulsation frequencies, we calculated the Fourier transform of the reduced light curve using the software PERIOD04 (Lenz & Breger 2005). When extracting the peaks, the light curve is fitted using the following formula:

$$m = m_0 + \Sigma A_i \sin(2\pi(f_i t + \phi_i)), \tag{1}$$

where m_0 is the zero-point, A_i is the amplitude of peak i, f_i is the corresponding frequency, and ϕ_i is the phase. We extracted the frequencies lower than 80 d^{-1}, which covers the typical pulsation frequency range of δ Sct stars. We iteratively subtracted frequencies from the data using Equ. 1 until the signal-to-noise ratio of the i^{th} peak was smaller than four (Breger et al. 1993). The uncertainties of frequencies were calculated following Montgomery & O'Donoghue (1999):

$$\sigma_f = 0.44 \frac{1}{T} \frac{1}{\mathrm{S/N}}, \tag{2}$$

where $T = 1035\,\mathrm{d}$ is the observation time span, and S/N is the signal-to-noise ratio of the peak. The noise is the average level within 2.5 c/d around the peak.

3.1. Pressure modes

Based on the Gaia EDR3 distance of 591 ± 11 pc (Bailer-Jones et al. 2021) and the apparent magnitude $V = 11.0$, we calculated the absolute magnitude to be $M_V = 2.14 \pm 0.04$ (neglecting extinction). Using the period–luminosity relation from Ziaali et al. (2019), we derive the expected the fundamental radial mode to be $13.86 \pm 0.43\,\mathrm{d}^{-1}$. The dominant frequency of $p_1 = 13.20362567(12)\,\mathrm{d}^{-1}$ is therefore consistent with the radial fundamental, especially given the intrinsic scatter in the P–L relation. In fact, if we assume a small amount of extinction ($A_V = 0.05$) then the P–L relation predicts the fundamental radial mode to be 13.3 ± 0.4 d^{-1}, in perfect agreement with the observed mode.

The fundamental radial p mode contributes the majority of the light variations. To see more details in the power spectrum, we removed the fundamental mode by the mean phased light curve shown in Fig. 1, and in Fig. 2 we display the amplitude spectrum of the residuals. We still can see the residual of the strongest fundamental mode with frequency $p_1 = 13.20362567(12)\,\mathrm{d}^{-1}$. As discussed in Sec. 5, these are sidelobes split by the obital frequency (Shibahashi & Kurtz 2012;

Shibahashi et al. 2015). We note that a peak appears at $p_2 = 17.003479(8)\,\mathrm{d}^{-1}$, with the ratio $p_1/p_2 = 0.7765$. Therefore, we identify the mode at p_2 as the first overtone. The second overtone is also found at $p_3 = 21.052996(7)\,\mathrm{d}^{-1}$ with the ratio $p_1/p_3 = 0.6272$. The conclusion of the p-mode frequencies and mode identifications are listed in Table 2.

Another stronger peak f_2 (=18.96664 d^{-1}) has a ratio of $p_1/f_2 = 0.696$, which is not equal to any value of the period ratios of the first four radial mode for δ Sct stars, i.e. p_1/p_2 (=0.756-0.787), p_1/p_3 (=0.611-0.632) and p_1/p_4 (=0.500-0.525), where p_1 is the frequency of the fundamental radial mode and p_2 to p_4 are the first, second and third overtones (Stellingwerf 1979; Netzel et al. 2021). Therefore, f_2 must belong to a non-radial mode. However, f_2 does not follow the typical échelle diagram discovered by Bedding et al. (2020), hence its mode identification is unclear.

3.2. Gravity modes

The modes with frequencies below $\sim 2.5\,\mathrm{d}^{-1}$, shown as the dark shaded area in Fig. 2, are below the typical frequency range of δ Sct stars. We also see the combinations between the fundamental radial mode p_1 and these low frequencies, marked by the light shaded areas in Fig. 2, which proves that they originate from the same star.

To identify these modes, we made the period échelle diagram for TIC 308396022, following the method described in Bedding et al. (2015) and Li et al. (2019). The result is shown in Fig. 3 and Table 3. It is clear that there is a vertical ridge with the period spacing ΔP about 2460 s that is within the typical range for dipole $l = 1$ g modes in γ Dor stars (Van Reeth et al. 2015, 2016; Li et al. 2019). We show the period spacing pattern in Fig. 4, and find that the period spacings ΔP fluctuate around 2500 s, but do not show a clear downward trend. The obvious fluctuation implies that the internal chemical composition gradients are large and the star is evolved to the terminal age main sequence (Miglio et al. 2008). Following the method by Van Reeth et al. (2016) and Li et al. (2019), we obtain the asymptotic spacing as $\Pi_0 = \sqrt{l(l+1)}\Delta P = 3655 \pm 13$ s, which

Table 2. The frequencies and the mode identifications of the fundamental p mode p_1, the first and the second overtones p_2, p_3.

Name	Frequency, d^{-1}	radial order	angular degree
p_1	13.20362567(12)	1	0
p_2	17.003479(8)	2	0
p_3	21.052996(7)	3	0

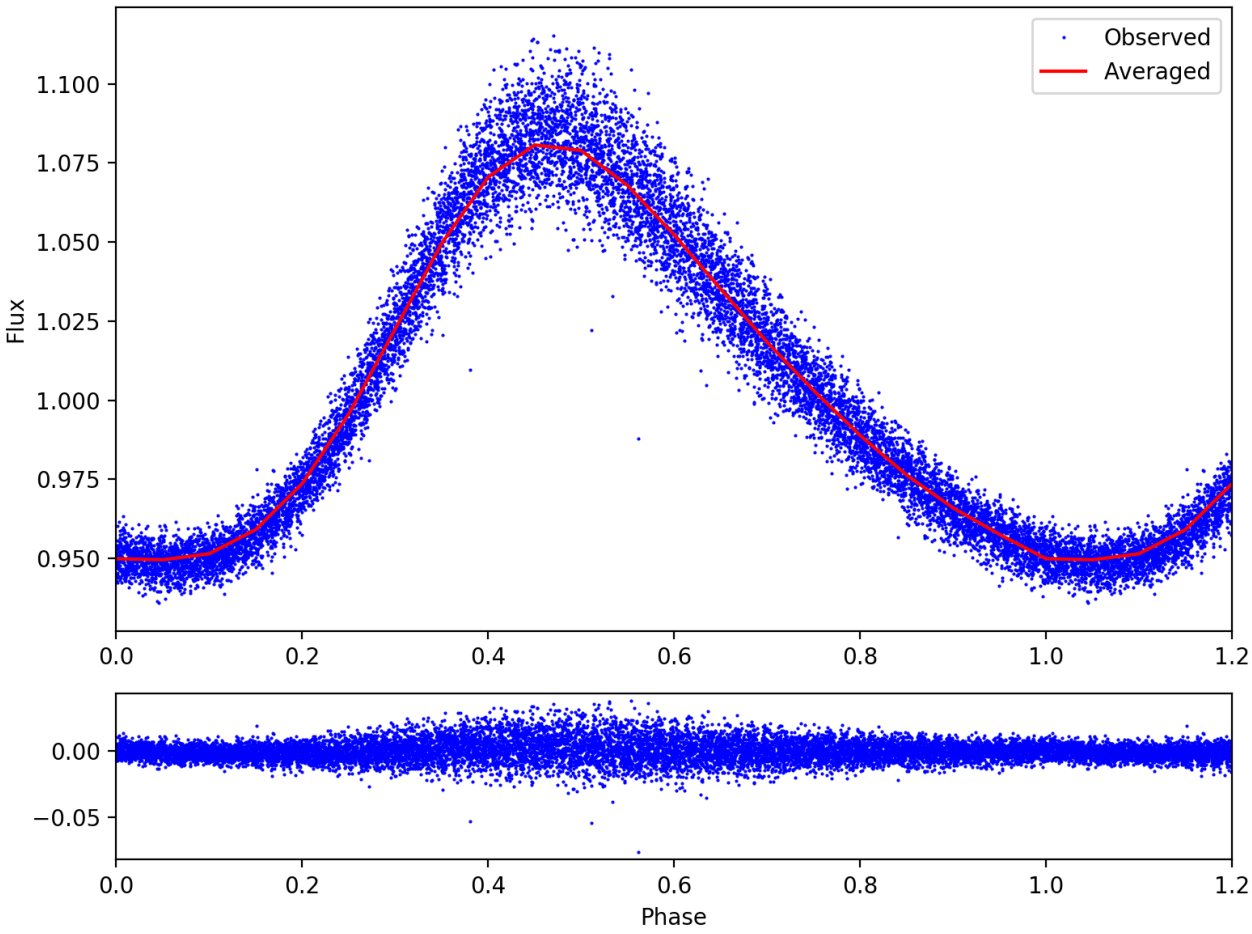

Fig. 1.— The phase diagram of TIC 308396022 from TESS data, folded by the frequency p_1 =13.20362567 d^{-1}. The obvious light variation of rapidly climbing and slow descent is typical for a HADS star.

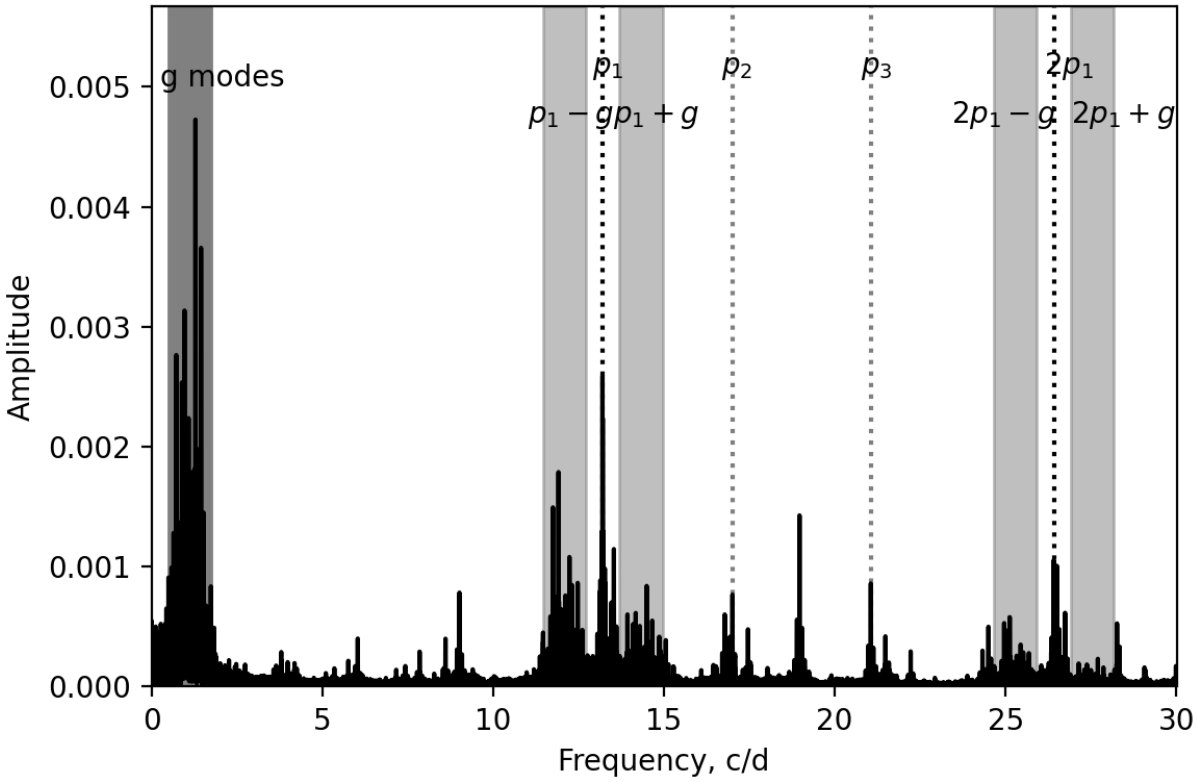

Fig. 2.— The amplitude spectrum of TIC 308396022, with the fundamental mode removed. The vertical dark-gray dotted line marks the location of the fundamental radial mode p_1, and the light-gray dotted lines mark the first and the second overtones, p_2 and p_3. The dark shaded area shows the g-mode region, while the light shaded areas around p_1 and $2p_1$ show the combinations between the fundamental p mode and the g modes: p_1+g, p_1-g, $2p_1+g$, and $2p_1-g$.

is smaller than the typical value of the γ Dor stars (about 4000 s, see Li et al. 2020). The small asymptotic spacing value also shows that this star has evolved to the end of the main sequence. However, the flat period spacing pattern indicates that the near-core rotation is slow, so that the effect of the Coriolis force is negligible (Bouabid et al. 2013). By the method from Van Reeth et al. (2016) and Li et al. (2019), we estimate the rotation rate as $0.006 \pm 0.003\,\mathrm{d}^{-1}$. Note that the slope in the $\Delta P - P$ relation is very small and it is strongly influenced by the scatter rather than the rotation effect, hence the rotation rate we give is imprecise. Slow-rotation is also consistent with the suggestion that the only difference between the HADS and small-amplitude δ Sct stars is the rotation rate (Xiong et al. 2016).

4. The location in the H-R Diagram

To investigate the evolutionary state of TIC 308396022, we calculated its luminosity as: L= 9.31 $\pm$ 0.50 $L_\odot$ (log $L/L_\odot$ = 0.97 $\pm$ 0.02) using the parameters from TIC (Stassun et al. 2018). Based on the luminosity log $L/L_\odot$ = 0.97 $\pm$ 0.02 and $T_{\rm eff}$ = 7371 $\pm$ 150 K from the TESS input catalogue, we plot the location of TIC 308396022 in the H-R Diagram shown in Fig. 5, as well as additional 34 well-studied HADS stars collected from literature (McNamara 2000; Poretti et al. 2005, 2011; Christiansen et al. 2007; Balona et al. 2012; Ulusoy et al. 2013; Peña et al. 2016; Yang et al. 2018; Yang 2019). From this figure, TIC 308396022 lies between of the δ Sct and the γ Dor instability strip and situate in the main sequence. We note that both the effective temperatures derived from *Gaia* and Antoci et al. (2019) are lower than that from TIC, which makes TIC 308396022 stand far apart from the HADS region and δ Sct instability strip.

5. Binary nature

By using the well-known 'Observed minus Calculated' ($O-C$) method (Sterken 2005), we measured the light maximum times of the fundamental p mode and found a significant time shift, as shown in Fig. 6. The light maximum times vary from −200 seconds to about 100 seconds, and the maxima of the $O-C$ diagram appear at about 1800 and 12000 cycles, leading to a period of around 800 days. We deduce that the periodic variation of the light maximum time is caused by the orbital motion of the pulsating star TIC 308396022, as observed in many previous large-amplitude variable stars (e.g. Fu & Sterken 2003; Conroy et al. 2014; Li et al. 2018).

To investigate the orbital parameters, we applied the phase-modulation method to the fundamental p mode p_1 and its harmonics $2p_1$, $3p_1$, and $4p_1$ (Murphy et al. 2014; Murphy & Shibahashi 2015; Murphy et al. 2016; Hey et al. 2020a,b), whose phase changes indicated the light travel

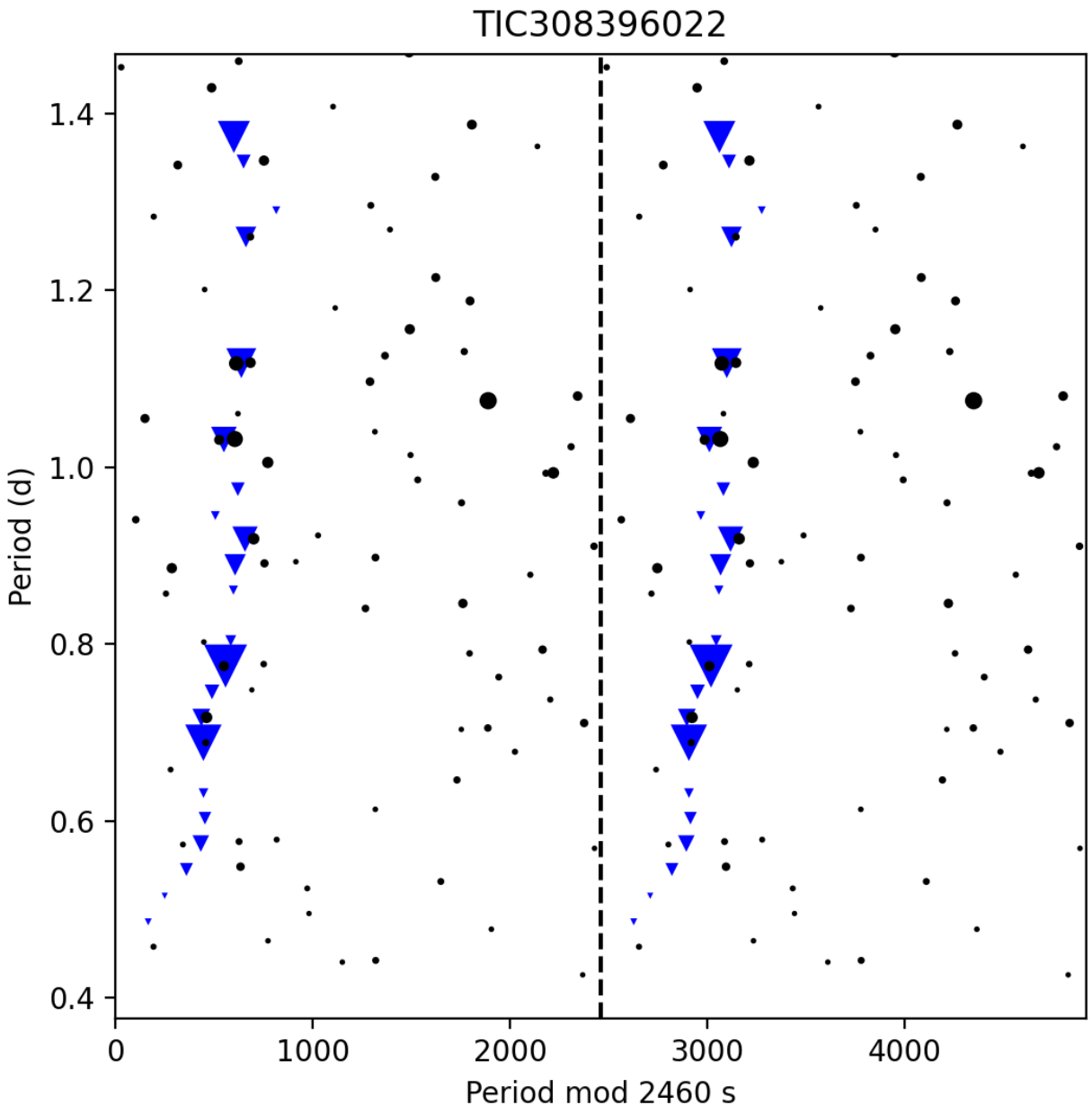

Fig. 3.— The period échelle diagram of TIC 308396022, showing a clear period spacing of about 2460 s. The blue triangles indicate g modes with l=1, while the black dots are probably noise peaks.

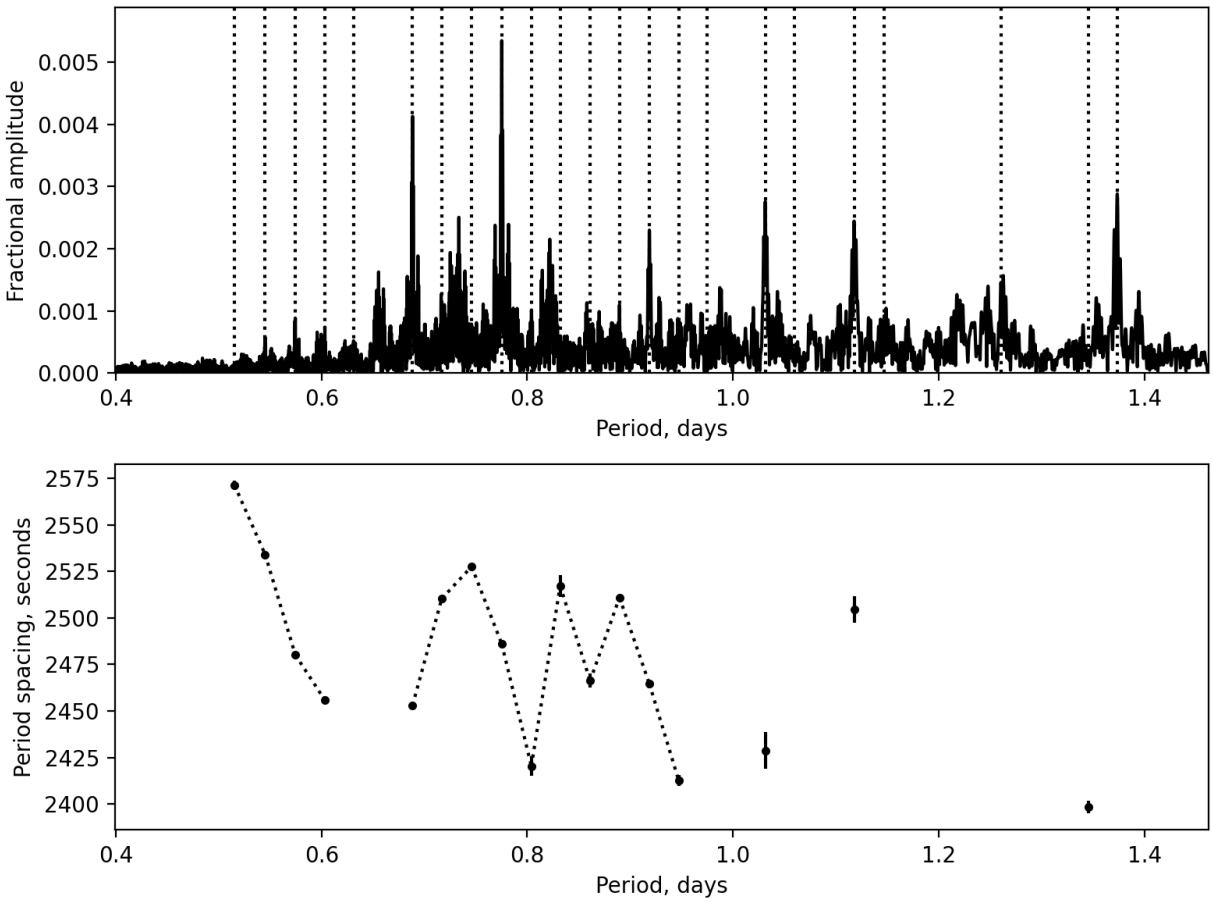

Fig. 4.— The amplitude spectrum and period spacing patterns of TIC 308396022. Upper panel: the amplitude spectrum with x-axis of period. The vertical dashed lines show the locations of the g modes in the period spacing patterns. Lower panel: the period spacing pattern. The dots are the period spacings between the adjacent modes.

Table 3. The g-mode frequencies and periods. The numbers in the brackets show the uncertainties in the last digits. The radial order is calculated by the period divided by the period spacing ΔP, which is set $\Delta P = 2460\,\mathrm{s}$.

Frequency, d^{-1}	Period, d	Radial order
2.05778(6)	0.485961(14)	17
1.94024(8)	0.515400(20)	18
1.834369(18)	0.545147(5)	19
1.740762(11)	0.574461(4)	20
1.657888(19)	0.603177(7)	21
1.58337(3)	0.631564(13)	22
1.4524286(23)	0.6885020(11)	24
1.394985(9)	0.716853(5)	25
1.340569(14)	0.745952(8)	26
1.2899600(16)	0.775218(10)	27
1.243789(25)	0.803995(16)	28
1.16131(4)	0.861095(26)	30
1.124017(7)	0.889666(5)	31
1.088470(5)	0.918721(4)	32
1.05770(4)	0.94545(3)	33
1.025381(16)	0.975247(15)	34
0.969583(5)	1.031371(5)	36
0.894606(3)	1.117810(4)	39
0.793373(7)	1.260441(11)	44
0.77478(5)	1.29069(8)	45
0.743097(15)	1.345720(28)	47
0.7280023(29)	1.373622(6)	48

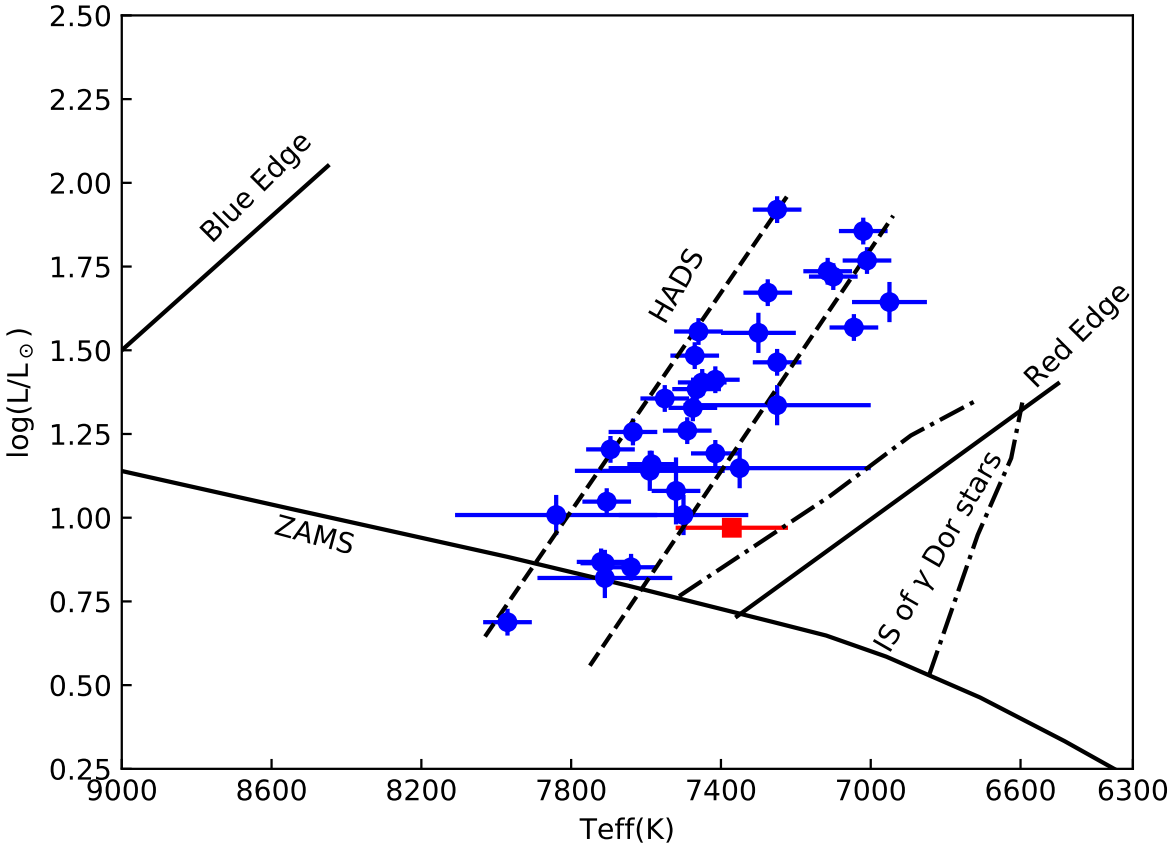

Fig. 5.— Location of the 34 well-studied HADS and TIC 308396022 in the H-R Diagram. TIC 308396022 is shown as the red square. The blue dots are the HADS collected from McNamara (2000); Poretti et al. (2005, 2011); Christiansen et al. (2007); Balona et al. (2012); Ulusoy et al. (2013); Peña et al. (2016); Yang et al. (2018); Yang (2019). The zero-age main sequence (ZAMS) and the δ Sct instability strip (solid lines) are from Murphy et al. (2019). The dashed lines show the region occupied by HADS, as found by McNamara (2000). The theoretical instability strip (IS) of γ Dor stars (dotted-dashed lines) is from Dupret et al. (2005).

effect is due to the orbital motion hence allow us to determine the orbital parameters. Figure 7 displays the time delay and the best-fitting model. The medians and one-sigma uncertainties from the positions of a Monte Carlo Markov Chain (MCMC) give the orbital period 803.5 ± 0.6 d, the projected semi-axis $a_1 \sin i/c = 262.9 \pm 1.2$ s, the eccentricity $e = 0.015 \pm 0.006$, and the mass function $f(M_1, M_2, \sin i) = \frac{(m_2 \sin i)^3}{(m_1+m_2)^2} = 0.0302 \pm 0.0004\,\mathrm{M}_\odot$.

The parameters of the orbit imply that the system might have undergone mass transfer (MT) and the secondary component might be a white dwarf (WD). When one of the two components of a binary system arrives at its asymptotic giant branch (AGB) stage, the radius of the expanding AGB star exceeds its Roche lobe and it starts mass-transfer to its companion (Lauterborn 1970; Karakas et al. 2000; Toonen et al. 2014). The orbit circularizes during the MT process and then the system leaves a post-AGB star, such as a blue straggler, a barium star, or a WD. Therefore, WDs are often found in a low-eccentricity system, and for A/F stars that are the primaries of systems in the period range detectable by *Kepler* (100-1500 d), 21% of the companions are WDs (Murphy et al. 2018). Assuming the mass of TIC 308396022 is $1.5\,\mathrm{M}_\odot$, the mass of the secondary is $0.49\,\mathrm{M}_\odot$ for the inclination $i = 90°$, or $0.58\,\mathrm{M}_\odot$ for $i = 60°$, which is within the typical mass range for a He WD.

We have calculated a coarse grid to model the star preliminarily using the stellar evolution code MESA (v12778, Paxton et al. 2011, 2013, 2015, 2018, 2019) and the stellar oscillation code GYRE (e.g. Townsend & Teitler 2013). The parameters of the grid were: mass from 1.4 to 2.2 solar masses with step of 0.1 solar masses, metallicity $Z = 0.020$, mixing length $\alpha = 2$ and exponential overshooting $f_{\rm ov} = 0.02$. The results are shown in Fig. 8, where the color represents the goodness-of-fit for the fundamental radial (p_1, left panel) and the g-mode asymptotic spacing (Π_0, right panel). We find that within the observation region ($T_{\rm eff} = 7371 \pm 150$ K, $\log L/L_\odot = 0.97 \pm 0.02$ derived in Section 4), there is no model that satisfies both the p- and g-mode pulsations. We also tried several other selections of metallicity, but still could not find a compatible model. The absence of the compatible model implies that the star has different core and envelope formation history, perhaps due to MT from the secondary star. Some recent research shows that asteroseismology has the ability to detect stellar merger or mass transfer in red giants (Rui & Fuller 2021; Deheuvels et al. 2021), and we suggest that TIC 308396022 might be the first main-sequence counterpart showing mass transfer by asteroseismology.

To confirm the history of the possible mass transfer, we propose two plans for future work:

- Performing detailed seismic modelling including the mass transfer from companions, since mass transfer may lead to incompatibility between the g- and p-mode pulsations and we cannot find a normal single-star evolution model that fits both the g and p modes in the same time;

- Conducting spectroscopic observations, which may help to indicate an enhancement of s-process elements which are created from the AGB donors.

6. Conclusions

We analyzed the pulsating behavior of TIC 308396022 by using the three-year photometric observations delivered from the TESS mission, and extracted p and g-mode pulsations from the 2-min cadence data with Fourier transform. The strongest peak $p_1 = 13.20362567(12)\,\mathrm{d}^{-1}$ is identified as the radial fundamental p mode, and we also detect the first overtone at $p_2 = 17.003479(8)\,\mathrm{d}^{-1}$ and the second overtone $p_3 = 21.052996(7)\,\mathrm{d}^{-1}$.

In the low-frequency region, we find an equally-spaced period pattern with the period spacing $\Delta P = 2460\,\mathrm{s}$. The asymptotic spacing is measured as $\Pi_0 = 3655 \pm 13\,\mathrm{s}$, lower than most of the γ Dor stars in Li et al. (2019). We propose that TIC 308396022 is the first HADS star with a g-mode period spacing pattern.

TIC 308396022 also shows clear orbital motion since its light maxima times and pulsation phases vary periodically. The orbit, which has a long period ($803.5 \pm 0.6\,\mathrm{d}$), a very small eccentricity (0.015), and a small mass function, indicates that the system probably has undergone MT and the companion is likely to be a He WD. Based on the derived luminosity $\log L/L_\odot = 0.97 \pm 0.02$, and the effective temperature $T_{\rm eff} = 7371 \pm 150\,\mathrm{K}$, TIC 308396022 lies near the bottom of the δ Sct instability strip. However, we were not able to find a theoretical model that matches the observed properties (L, T_{eff}, $p_1$and Π_0). Spectroscopic observations and detailed evolutionary–seismic modellings considering the mass accretion are needed to reveal the history of this system further.

This research is supported by the program of the National Natural Science Foundation of China (grant Nos. 11573021, U1938104 and 12003020). Gang Li acknowledges support from the project BEAMING ANR-18-CE31-0001 of the French National Research Agency (ANR) and from the Centre National d'Etudes Spatiales (CNES). We are grateful to the Australian Research Council for support (DP 210103119). This work has made use of data from the European Space Agency (ESA) mission *Gaia* (https://www.cosmos.esa.int/gaia), processed by the *Gaia* Data Processing and Analysis Consortium (DPAC, https://www.cosmos.esa.int/web/gaia/dpac/consortium). Funding for the DPAC has been provided by national institutions, in particular the institutions participating in the *Gaia* Multilateral Agreement. We would like to thank the TESS science team for providing such excellent data.

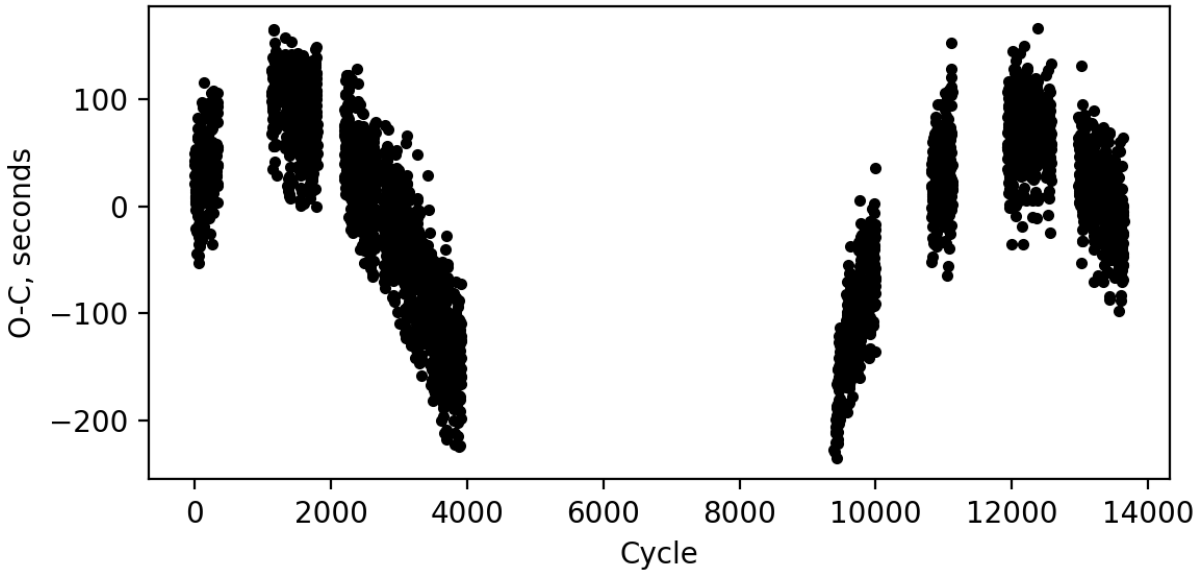

Fig. 6.— The $O-C$ diagram of TIC 308396022, based on the dominant pulsation mode (p_1).

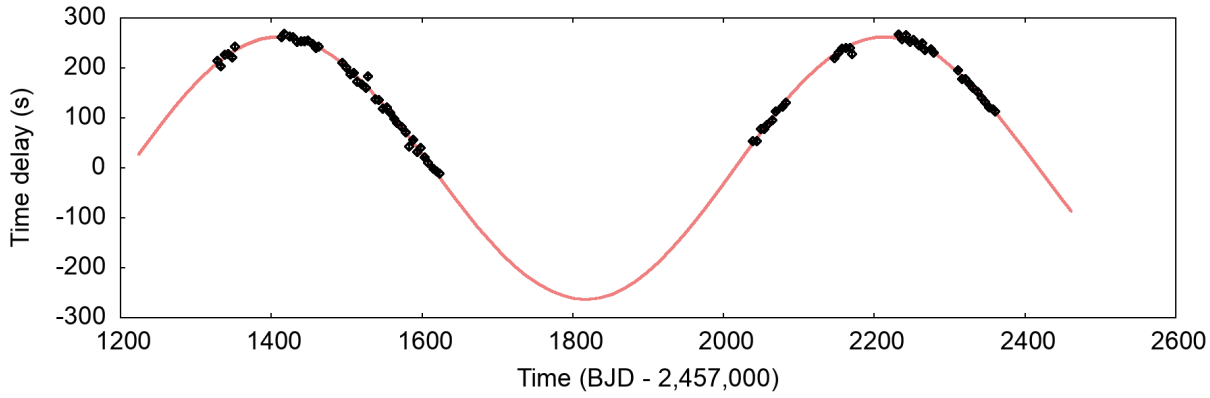

Fig. 7.— Time delay measurements (black symbols) for TIC 308396022, using 10-d light curve segments. Red curves show 25 random samples from the Markov chain.

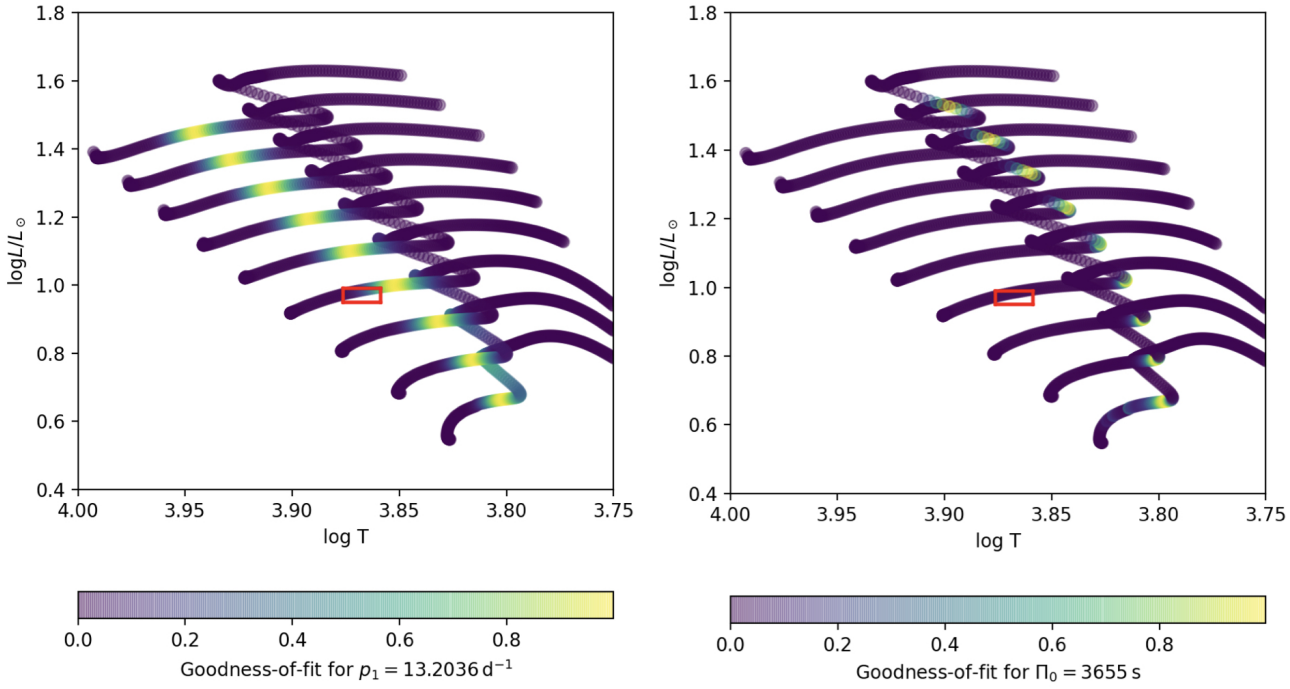

Fig. 8.— The comparison between the observations and models with $Z = 0.020$, mixing length $\alpha = 2$, and exponential overshooting $f_{\rm ov} = 0.02$. The mass is from 1.4 to 2.2 solar masses with steps of 0.1 solar masses. The red box shows the observed region ($T_{\rm eff} = 7371 \pm 150\,\mathrm{K}$, $\log L/L_\odot = 0.97 \pm 0.02$), and the color shows the goodness-of-fit for the fundamental radial (p_1, left) and asymptotic spacing (Π_0, right).

REFERENCES

Aerts, C., Christensen-Dalsgaard, J., & Kurtz, D. W. 2010, Asteroseismology, Astronomy and Astrophysics Library. ISBN 978-1-4020-5178-4. Springer Science+Business Media B.V., 2010, p.

Aerts, C. 2021, Reviews of Modern Physics, 93, 015001.

Antoci, V., Cunha, M. S., Bowman, D. M., et al. 2019, MNRAS, 490, 4040

Bailer-Jones, C. A. L., Rybizki, J., Fouesneau, M., et al. 2021, AJ, 161, 147.

Baglin, A., Auvergne, M., Barge, P., et al. 2009, Transiting Planets, 253, 71.

Balona, L. A. and Krisciunas, K. & Cousins, A. W. J., 1994, MNRAS, 270, 905-913

Balona L. A., Lenz P., Antoci V., et al., 2012, MNRAS, 419, 3028-3038

Bedding, T. R., Murphy, S. J., Colman, I. L., et al. 2015, European Physical Journal Web of Conferences, 101, 01005.

Bedding, T. R., Murphy, S. J., Hey, D. R., et al. 2020, Nature, 581, 147.

Borucki W. J., Koch D., Basri G., et al., 2010, Science, 327, 977

Bouabid, M.-P., Dupret, M.-A., Salmon, S., et al. 2013, MNRAS, 429, 2500.

Bowman, D. M. 2017, Amplitude Modulation of Pulsation Modes in Delta Scuti Stars, Springer Theses series. ISBN 978-3-319-66649-5. Springer International Publishing, 2017.

Bowman, D. M. & Kurtz, D. W. 2018, MNRAS, 476, 3169.

Bradley, P. A., Guzik, J. A., Miles, L. F., et al. 2015, AJ, 149, 68.

Breger M., Stich J., Garrido R., et al. 1993, A&A, 271, 482

Breger, M. & Beichbuchner, F. 1996, A&A, 313, 851

Breger M., 2000, Delta Sciti and Related Stars ASP Conf Series, 210, 3

Catelan, M. & Smith, H. A. 2015, Pulsating Stars (Wiley-VCH), 2015

Chaplin, W. J. & Miglio, A. 2013, ARA&A, 51, 353.

Christiansen, J. L., Derekas, A., Ashley, M. C. B., et al., 2007, MNRAS, 382, 239

Conroy, K. E., Prša, A., Stassun, K. G., et al. 2014, AJ, 147, 45.

Deheuvels, S., Ballot, J., Gehan, C., et al. 2021, arXiv:2108.11848

Dupret, M.-A., Grigahcène, A., Garrido, R., et al. 2004, A&A, 414, L17.

Dupret, M.-A., Grigahcène, A., Garrido, R., et al. 2005, MNRAS, 360, 1143.

Dupret, M.-A., Grigahcène, A., Garrido, R., et al. 2005, A&A, 435, 927.

Drilling, J. S. & Landolt, A. U. 2000, Allen's Astrophysical Quantities, 381

Fu, J. N. & Sterken, C. 2003, A&A, 405, 685.

Gaia Collaboration, Brown, A. G. A., Vallenari, A., et al. 2016, A&A, 595, A2.

Gaia Collaboration, Brown, A. G. A., Vallenari, A., et al. 2018, A&A, 616, A1.

Grigahcène, A., Antoci, V., Balona, L., et al. 2010, ApJ, 713, L192.

Goupil, M.-J., Dupret, M. A., Samadi, R., et al. 2005, Journal of Astrophysics and Astronomy, 26, 249.

Guzik, J. A., Kaye, A. B., Bradley, P. A., et al. 2000, ApJ, 542, L57.

Handler, G. & Shobbrook, R. R. 2002, MNRAS, 333, 251.

Handler, G. 2009, MNRAS, 398, 1339.

Handler, G. 2009, Stellar Pulsation: Challenges for Theory and Observation, 1170, 403.

Handler, G. 2013, Planets, Stars and Stellar Systems. Volume 4: Stellar Structure and Evolution, 207.

Hareter, M., Reegen, P., Miglio, A., et al. 2010, arXiv:1007.3176

Henry, G. W. & Fekel, F. C. 2005, AJ, 129, 2026.

Hey, D. R., Murphy, S. J., Foreman-Mackey, D., et al. 2020, AJ, 159, 202.

Hey, D., Murphy, S., Foreman-Mackey, D., et al. 2020, The Journal of Open Source Software, 5, 2125.

Holdsworth, D. L., Smalley, B., Gillon, M., et al. 2014, MNRAS, 439, 2078.

Karakas, A. I., Tout, C. A., & Lattanzio, J. C. 2000, MNRAS, 316, 689.

Kaye, Anthony B. and Handler, Gerald and Krisciunas, Kevin and Poretti, Ennio and Zerbi, Filippo M., 1999, PASP, 111, 840

Kurtz, D. W., Saio, H., Takata, M., et al. 2014, MNRAS, 444, 102.

Lauterborn, D. 1970, A&A, 7, 150

Lenz P., Breger M. 2005, CoAst, 146, 53

Li, G., Fu, J., Su, J., et al. 2018, MNRAS, 473, 398.

Li, G, Van Reeth, T, Bedding, T, R., Murphy, S, J., Antoci, V., 2019b, MNRAS, 487, 782.

Li, G., Bedding, T. R., Murphy, S. J., et al. 2019, MNRAS, 482, 1757.

Li, G., Van Reeth, T., Bedding, T. R., et al. 2020, MNRAS, 491, 3586.

Lomb, N. R. 1976, Ap&SS, 39, 447.

Maeder, A. 2009, Physics, Formation and Evolution of Rotating Stars: , Astronomy and Astrophysics Library. ISBN 978-3-540-76948-4. Springer Berlin Heidelberg, 2009.

Mamajek, E. E., Torres, G., Prsa, A., et al. 2015, arXiv:1510.06262

McDonald, I., Zijlstra, A. A., & Watson, R. A. 2017, MNRAS, 471, 770

McNamara D. H., 2000, in Delta Scuti and Related Stars,. M. Breger, & M. H. Montgomery, ASP Conf.Ser., 210, 373

Miglio, A., Montalbán, J., Noels, A., et al. 2008, MNRAS, 386, 1487.

Montgomery M. H., & O'Donoghue D., 1999, Delta Scuti Star Newsletter, 13, 28

Moya, A., Suárez, J. C., Amado, P. J., et al. 2005, A&A, 432, 189.

Murphy, S. J., Bedding, T. R., Shibahashi, H., et al. 2014, MNRAS, 441, 2515.

Murphy, S. J. & Shibahashi, H. 2015, MNRAS, 450, 4475.

Murphy, S. J., Shibahashi, H., & Bedding, T. R. 2016, MNRAS, 461, 4215.

Murphy, S. J., Moe, M., Kurtz, D. W., et al. 2018, MNRAS, 474, 4322.

Murphy, S. J., Hey, D., Van Reeth, T., et al. 2019, MNRAS, 485, 2380.

Netzel, H., Pietrukowicz, P., Soszyński, I., et al. 2021, arXiv:2107.08064

Ouazzani, R.-M., Salmon, S. J. A. J., Antoci, V., et al. 2017, MNRAS, 465, 2294.

Ouazzani, R.-M., Lignières, F., Dupret, M.-A., et al. 2020, A&A, 640, A49.

Paxton, B., Bildsten, L., Dotter, A., et al. 2011, ApJS, 192, 3.

Paxton, B., Cantiello, M., Arras, P., et al. 2013, ApJS, 208, 4.

Paxton, B., Marchant, P., Schwab, J., et al. 2015, ApJS, 220, 15.

Paxton, B., Schwab, J., Bauer, E. B., et al. 2018, ApJS, 234, 34.

Paxton, B., Smolec, R., Schwab, J., et al. 2019, ApJS, 243, 10.

Peña, J. H., Villarreal, C., Piña, D. S., et al., 2016, RMxAA, 52, 385

Petersen, J. O. 1989, Delta Scuti Star Newsletter, vol. 1, p.6, 1

Petersen, J. O. & Christensen-Dalsgaard, J. 1996, A&A, 312, 463

Poretti, E., Suárez, J. C., Niarchos, P. G., et al., 2005, A &A, 440, 1097

Poretti, E., Rainer, M., Weiss, W. W., et al., 2011, A & A, 528, A147

Prša, A., Harmanec, P., Torres, G., et al. 2016, AJ, 152, 41.

Ricker, G. R., Winn, J. N., Vanderspek, R., et al. 2014, Proc. SPIE, 9143, 914320.

Ricker, G. R., Winn, J. N., Vanderspek, R., et al. 2015, Journal of Astronomical Telescopes, Instruments, and Systems, 1, 014003.

Rui, N. Z. & Fuller, J. 2021, arXiv:2108.10322

Saio, H., Kurtz, D. W., Takata, M., et al. 2015, MNRAS, 447, 3264.

Saio, H., Takata, M., Lee, U., et al. 2021, MNRAS, 502, 5856.

Scargle, J. D. 1982, ApJ, 263, 835.

Shibahashi, H. 1979, PASJ, 31, 87

Shibahashi, H. & Kurtz, D. W. 2012, MNRAS, 422, 738.

Shibahashi, H., Kurtz, D. W., & Murphy, S. J. 2015, MNRAS, 450, 3999.

Smeyers, P. & Moya, A. 2007, A&A, 465, 509.

Stassun, K. G., Oelkers, R. J., Pepper, J., et al. 2018, AJ, 156, 102.

Stellingwerf, R. F. 1979, ApJ, 227, 935

Sterken, C. 2005, The Light-Time Effect in Astrophysics: Causes and cures of the O-C diagram, 335, 3

Tassoul, M. 1980, ApJS, 43, 469.

Townsend, R. H. D. 2005, MNRAS, 360, 465.

Townsend, R. H. D. & Teitler, S. A. 2013, MNRAS, 435, 3406.

Toonen, S., Voss, R., & Knigge, C. 2014, MNRAS, 441, 354.

Uytterhoeven, K., Moya, A., Grigahcène, A., et al. 2011, A&A, 534, A125.

Ulusoy, C., Ulaş, B., Gülmez, T., et al., 2013, MNRAS, 433, 394

Van Reeth, T., Tkachenko, A., Aerts, C., et al. 2015, ApJS, 218, 27.

Van Reeth, T., Tkachenko, A., & Aerts, C. 2016, A&A, 593, A120.

Xiong, D. R., Deng, L., Zhang, C., et al. 2016, MNRAS, 457, 3163.

Yang T. Z., Esamdin A., Fu J. N., et al., 2018, RAA, 18, 2

Yang, T., Esamdin, A., Song, F., et al. 2018, ApJ, 863, 195.

Yang T. Z., & Esamdin A., 2019, ApJ, 879, 59Y

Ziaali, E., Bedding, T. R., Murphy, S. J., et al. 2019, MNRAS, 486, 4348.